A cohesive model for ice and its verification with tensile splitting tests

Hauke Herrnring, Leon Kellner, Jan M. Kubiczek, Sören Ehlers

Technische Universität Hamburg

1 Introduction

Ships and offshore structures operating in areas such as the Arctic have to be designed to withstand ice induced loads, e.g. from ice floe impact. This is mostly done with empirical methods, which have several drawbacks, e.g. they only give upper estimates of global loads. Numerical simulations of ice interaction are a desirable remedy, but their accuracy is currently limited if the material model doesn't account for fracture processes. One approach is to use an elastic bulk material model along with the cohesive zone method (CZM) to model all inelastic deformation, i.e. fracture. Here, this approach is applied to simulate tensile splitting tests. The focus is on parameter identification and numerical instabilities for fine discretizations.

To be more specific, ice-loads are significant for the design of maritime structures operating in areas with at least seasonal ice coverage. Brittle ice structure interaction (ISI) is dominated by fracture in the form of multiple interacting cracks and approximately elastic bulk behavior. However, modeling fracture and the verification of such models remains a challenge, particularly for ice. Often, fracture is not modeled, [1, 2], or elements that reach failure are simply deleted [3, 4] which lacks physical explanation. Detailed models do exist, e.g. [5, 6], but have only been applied to uniaxial simulations or don't capture behavior after initial failure.

One reason for shortcomings of fracture models is the lack of suitable verification experiments. The majority of experimental data is from compression experiments [7]. However, fracture is usually not initiated under pure compression or hydrostatic stress states. Rather, cracks occur as a result of tensile and shear stresses, which can originate from global compression stress, e.g. through wing cracks [8]. Before tackling a complex fracture process such as wing cracks, fracture models should be verified with straightforward tensile and shear stress states. For such stress states, current options for experimental verification are mostly uniaxial tensile and single crack beam tests, see e.g. [9–11]. Other experiments with biaxial stress states, such as tensile splitting tests, are desirable but rarely done, see e.g. [12].

With respect to the fracture model, the CZM is applied. The method is straightforward to implement in existing finite element models and a good compromise between precision and efficiency. Drawbacks of the CZM are various known numerical issues, [9, 13], which get worse for finer meshes. Further challenges are the identification of suitable material parameters and the model calibration and verification, respectively.

Regarding the numerical issues, bounds for parameters and their interdependency are shown for different meshes. Aspects such as the cohesive element stiffness, traction and damage process are discussed in view of element size and physics based constraints.

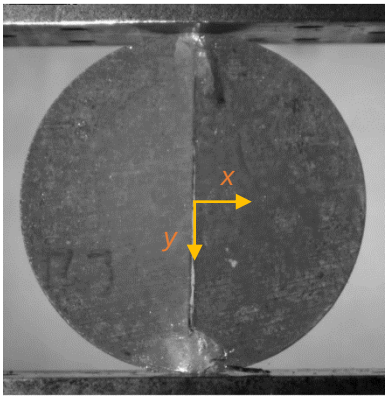

Figure 1 - Tensile splitting test in ice with vertical crack

Regarding the verification, tensile splitting- or Brazilian tests (TST) are suggested as an alternative to uniaxial tensile tests. This method is common for the characterization of brittle materials such as rocks. A solid disc is diametrically compressed. In theory, in the center, the material undergoes biaxial tension to failure. The sample preparation and conducting of tests is simple. TSTs are not suitable for determining the tensile strength of ice [14]. Nevertheless, the TST represents a valuable possibility to verify tension-dominated failure through experimental observations and corresponding numerical analysis.

In a nutshell, two key issues are subject of this paper:
(i) the modeling of fracture in ice with the CZM and resulting numerical instabilities, particularly for fine meshes and
(ii) the comparison of fracture models to experiments.

2 Application of the cohesive zone model to fracture in ice

2.1 Tensile splitting tests

Tensile tests for brittle materials are challenging. An alternative is the tensile splitting test or Brazilian test. Tensile splitting is a standardized test method for the characterization of materials such as rock [15] or concrete [16]. The specimen production and test conduction of the tensile splitting tests are easier in comparison to conventional tensile tests. However, previous investigations have shown that the test is only conditionally suitable for determining the tensile strength of ice [14]. As a benchmark for the CZM simulations shown here, tensile splitting tests with fine grained fresh water ice were carried out. The diameter of the disc specimens is 99.4 mm and the thickness is 20 mm. Eleven experiments with a nominal crosshead speed of 10 mm/s and plane steel plates were chosen as a compromise between computing time and the lowest possible dynamic effects. The mean force of this group is 1.3 kN with a standard deviation of 0.22 kN. All experiments were recorded with a high-speed camera. After a short loading time, microcracks formed in the contact area between the ice and the loading plates. Brittle failure was observed for all samples. A vertical crack grew through the sample, see also Figure 1.

2.2 Preliminaries

2.2.1 The bulk model

The approach to modeling brittle ice behavior combines a bulk material model with the cohesive zone method (CZM) as described in [17]. Here, a simple isotropic elastic bulk material model **MAT_PLASTIC_KINEMATIC** was used, as **MAT_ELASTIC** is only valid for small finite strains. A homogeneous bulk response is implicitly assumed. To the authors' knowledge, there exists no general criterion yet regarding the number of grains necessary to homogenize three dimensional bulk behavior of ice. Numerically, it was shown in two dimensions that 230 grains are required for homogeneous elastic behavior of polycrystalline ice, which corresponds to 15 times the average grain diameter [18]. This agrees with recommendations for experiments [19]. The grain diameter of the ice used in the tensile splitting tests was $\sim 2\ \mathrm{mm}$. Therefore the required minimum element size would be $30\ \mathrm{mm}$, which is too big for a model (and specimen) size with a diameter of $100\ \mathrm{mm}$. Hence the assumption of a homogeneous response cannot be upheld. This simplification probably affects the results, but the magnitude of the effect is not known at present [5].

2.2.2 The cohesive zone method

To apply the CZM, the parameters for the traction separation law (TSL) have to be identified and several numerical issues have to be addressed. The following parameters are needed: the cohesive element stiffness, i.e. initial slope of the curve, the maximum traction and the energy release rate.
Usually, the TSL parameters are not known in advance and have to be back calculated by comparing simulation and experiment [20–22]. For biaxial stress states, back calculation is not straightforward, since other aspects might influence the outcome. More research is needed.
Therefore, parameters from previous work based on a simple comparison to a uniaxial tensile test were adopted, see [9] and [10], respectively. The uniaxial tensile test was used as a reference because the ice in the tensile splitting experiment is expected to fail under tension.
The energy release rate (ERR) was chosen as $G = 4\ \mathrm{Jm}^{-2}$. This value might be too high, because the ERR possibly decreases with decreasing specimen size [19, 23] and the specimens here are smaller than for the reference experiment. Yet conclusions regarding the ERR on small scales $\lesssim 1\mathrm{m}$ are premature and this value is considered sufficiently realistic.
Next, a maximum traction value has to be determined. Generally, (global) tensile strength increases for smaller specimens in bending [24]. For true uniaxial tensile tests data is not sufficient to reach conclusions, e.g. [25], but the same size effect is expected. The tractions used are given in Table 1.
The choice of initial stiffness, i.e. initial slope of the TSL, is guided by numerical considerations rather than physics. Using cohesive elements with initial stiffness introduces artificial compliance to the model. This is also influenced by element size [13]. There are different approaches to tackle this issue. A common solution is using a high initial stiffness. In explicit solvers this approach is limited because the time step is influenced by the stiffness. A good compromise can be found with an approach based on minimal one-dimensional models [9].
Lastly, the length of the cohesive zone has to be estimated. This can be done with various formulas, typically given for plane stress or plane strain conditions. The calculated cohesive zone length may vary significantly for different formulas. Here, it was estimated for brittle fracture and plane stress according to [26, 27].

$$l_{cz} = \frac{9\pi}{32} E \left(\frac{G}{\tau^2}\right) \quad (2)$$

This length is compared to the average element length. There is no universally agreed minimum number of elements in the cohesive zone. Suggestions range from 2 to 10 elements [26, 28]. In general, a finer discretization is desirable and also often needed to satisfy the requirement of more than two elements in the cohesive zone.

Once the necessary TSL parameters are calculated, the homogeneous elastic behavior of bulk and cohesive elements requires double-checking. The reason is that the elastic parameters are estimated with 1-D 'back-of-the-envelope' formulas that neglect 3-D mesh characteristics. Lower bounds for the homogenized, overall Young's modulus and Poisson's ratio are calculated following the work by Blal et al. They employ a 3-D matrix-inclusion composite to derive theoretical criteria on cohesive parameters [29]. First, the ratio of homogenized modulus E_{hom} to the desired target modulus of ice E_{target} is calculated as

$$\frac{E_{\mathrm{hom}}}{E_{\mathrm{target}}} = \frac{\xi_{\mathrm{E}}}{1 + \xi_{\mathrm{E}}} \quad (3)$$

$$\xi_{\mathrm{E}} = \frac{5}{1 + \frac{4}{3} \cdot \frac{E_{\mathrm{N}}}{E_{\mathrm{T}}}} \cdot \frac{E_{\mathrm{N}}}{E_{\mathrm{b}} Z} \quad (4)$$

This approach includes the cohesive normal and tangential stiffnesses E_{N} and E_{T} and the ratio of cohesive element area to bulk element volume

$$Z = \frac{A_{\mathrm{coh}}}{V_{\mathrm{bulk}}} \quad (5)$$

The ratio $E_{\mathrm{hom}}/E_{\mathrm{target}}$ should be as close to one as possible. Crucially, the Z ratio increases for finer meshes and lowers ξ_{E} which in turn makes it difficult to achieve this.

Secondly, the ratio of homogenized, overall Poisson's ratio ν_{hom} to the desired target Poisson's ratio ν_{target} is calculated as

$$\frac{\nu_{\mathrm{hom}}}{\nu_{\mathrm{target}}} = \frac{E_{\mathrm{b}} Z \left(-1 + 2\frac{E_{\mathrm{N}}}{E_{\mathrm{T}}}\right) + 15 E_{\mathrm{N}} \nu_{\mathrm{b}}}{E_{\mathrm{b}} Z \left(3 + 4\frac{E_{\mathrm{N}}}{E_{\mathrm{T}}}\right) \nu^{M} + 15 E_{\mathrm{N}} \nu_{\mathrm{b}}} \quad (6)$$

Overall, the aim is to achieve ratios ≥ 0.95. These ratios and parameters are only valid for the TSL up to the point of damage initiation or crack propagation, respectively.

Besides the TSL parameters, the mass of the cohesive elements is an issue. Although the cohesive elements are virtually two-dimensional, they are assigned either (i) a thickness of one distance unit (in our case $1\ \mathrm{m}$) in LS-Dyna and a density per volume or (ii) a density per area. Hence the cohesive elements add mass to the model. This is corrected by distributing the total mass between the cohesive and bulk elements, e.g. [9].

Finally, it is emphasized that it is not straightforward to establish a consistent set of parameters for the CZM due to several numerical as well as physics based restrictions. Upper and lower boundaries of parameters are shown in Figure 2. Regarding the ERR G, a high value results in ductile behavior whereas a value too low would be unphysical, since cracks have to release energy. The cohesive element stiffnesses should be as high as possible to decrease artificial compliance and meet target elastic ratios (Eqs. 3 and 6). However, very high values lead to a small time step size and numerical instabilities. The normal traction σ needs to be chosen such that simulations can represent tensile tests. The ratio τ/σ is not known for ice, but the ratio for rock as another highly brittle material is about two [5]. Lastly, if the element size is too big, the requirement of 2-3 elements in the cohesive zone is not met, whereas for very small element sizes time step size decreases. As mentioned, small elements increase the Z ratio which makes it harder to fulfill the requirements on the E, ν ratios (Eqs. 3 and 6). Balancing and discussing these interdependencies is a key issue in this paper.

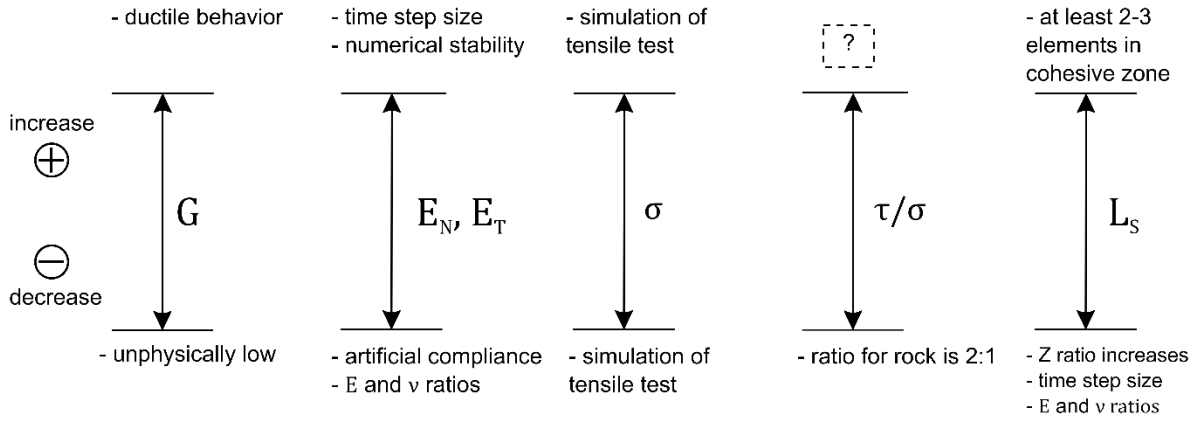

Figure 2 - Numerical and physical boundaries of parameters

2.2.3 Contact and element formulation

For all parts the ***ERODING_SINGLE_SURFACE** contact was used. This way the different parts of the fractured specimen can still come into contact, as is the case in the experiments. Unfortunately, it is not possible yet to use tetrahedron elements to model 3-D fracture. The reason is that an ***ERODING_SINGLE_SURFACE** contact is required to prevent contact between bulk elements prior to failure of the cohesive elements. If this is not enabled, only a fraction of the stress between two bulk elements actually reaches the cohesive element. Therefore, structured hexahedron meshes were used in all simulations.

3 Results

3.1 Validation

3.1.1 Elasticity

Before verifying the simulation against the experiment, the key assumptions and elastic parameters have to be validated. For this, the results for the models with and without cohesive elements were compared for a bent contact surface. Ideally, the elastic response in terms of force and stress fields are the same. Figure 3 indicates the force between steel plates and specimen for different element sizes L_S and cohesive/no cohesive models. For the case “no CZM hex 0.0025”, the contact algorithm caused initial force oscillations that faded after about $20\ \mathrm{ms}$. For the finer meshes, the slope of the force curve increased after about $45\ \mathrm{ms}$ which is probably owed to the better discretization and the bent contact geometry. Nevertheless, overall the curves match.

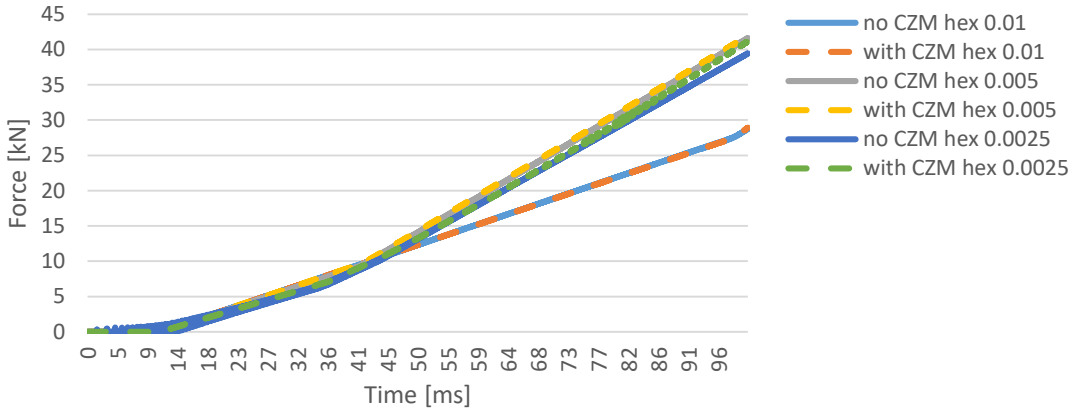

Figure 3 – Simulated force over time between steel plate and ice specimen for different discretizations and modesl with and without cohesive elements inserted

Figure 4 indicates the x-stress over x-coordinate, i.e. the stress normal to the fracture path on a path parallel to that stress. Again, stresses are shown for different discretizations and cohesive/no cohesive. The coarse mesh does not accurately resolve the stress, but overall the CZM / no CZM stresses match.

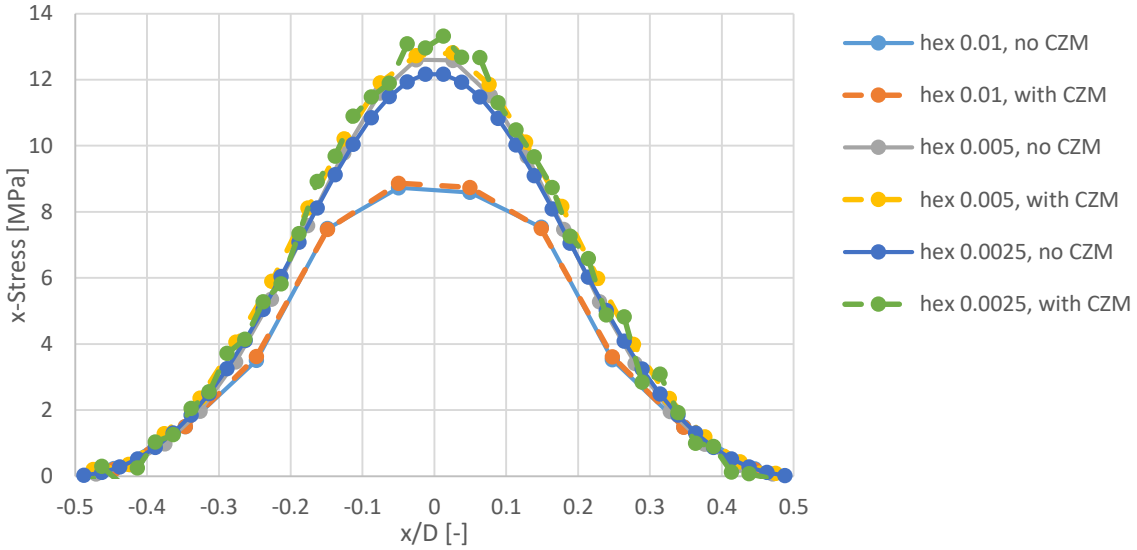

Figure 4 – X-stress evaluated over x-coordinate in the middle of the disc, i.e. over a path crossing the disc, see Figure 1 for coordinate system.

Remarkably, the green curve (hex 0.0025, with CZM) is not as smooth as expected. Apparently the cohesive elements slightly distort the stress field for the fine mesh. All in all, the elastic behavior for models with and without cohesive elements is almost identical.

3.1.2 Numerical instability

The models with cohesive elements were prone to numerical instabilities, particularly the model with the fine mesh. In many cases, all cohesive elements were suddenly deleted which resulted in an explosion-like model behavior. This was often preceded by irregular fracture patterns. The key issues identified were: (i) the required high initial stiffness of the cohesive elements, (ii) the ratio of normal to tangential traction, (iii) a high contact stiffness, and (vi) possibly the damage process.
Regarding (i), it is known that a high initial stiffness causes numerical problems. Decreasing the stiffness helps. Yet the fine mesh prescribes lower bounds for the stiffness in order to not violate (Eqs. 3 and 6). The ratio of normal to tangential traction, issue (ii), was also critical. A relatively high tangential traction or neglecting failure due to tangential separation partially alleviated the instabilities. With respect to the contact stiffness (iii), a fine mesh decreases the time step which in turn increases the contact stiffness. This can lead to a high contact stiffness, which probably causes problems similar to the high initial stiffness of the cohesive elements.
Lastly, issue (vi), the damage process implemented in ***MAT_COHESIVE_MIXED_MODE** causes softening. Depending on the fracture path and stress field this may result in undamaged and very stiff elements which are in the neighborhood of elements with almost zero stiffness. Consequently, it was only possible to run models with ***MAT_COHESIVE_ELASTIC** which does not include any damage process and an unphysically low ratio of normal to tangential traction. In other words, cohesive element failure due to tangential stress was not possible.
In Table 1, mesh related parameters are shown for different element lengths. The Z-ratio decreases with smaller elements whereas the cohesive element stiffness increases. For structured meshes this increase is linear. The ratios for the elastic moduli should be above 0.95, but are considered sufficient. Furthermore, it is recommended that $\xi_E \geq 20$, which is not reached [29]. Nonetheless, this does not negatively impact the coarser mesh models. However, there appears to be a threshold for Z or ξ_E values over which numerical instabilities are likely to occur.
In short, the small element size caused several issues due to decrease in time step and stiffness of the cohesive element and contact, respectively.

Table 1 - Parameters of the cohesive method

Description or equation	Symbol	Unit	Values		
Element length	L_s	m	0.0025	0.005	0.01
Density cohesive elements	ρ_{CZM}	kg/m³	0.366	0.75	1.5
Z-ratio	Z	m^-1	1230	579	253
Eq.4	ξ_E	m	13.2	14.1	16.1
E-ratio	E_{hom}/E_t	-	0.93	0.93	0.94
ν-ratio	ν_{hom}/ν_t	-	0.96	0.96	0.97
Corrected bulk modulus	E_{bc}	Pa	1E10	1E10	1E10
Poisson's ratio	ν_b	-	0.33	0.33	0.33
Cohesive element stiffness	E_{CZM}	Pa/m	3.60E+13	1.80E+13	9.00E+12
Maximum traction mode I	T	Pa	3.60E6	2.25E6	1.15E6

3.2 Verification

For verification, three models with different mesh sizes were simulated. The fracture in all simulations initiated in the contact area between steel and ice specimen. Subsequently the crack ran vertically through the specimen. The same behavior is observed in experiments, see Figure 1 and Figure 5. Initially, microcracks appeared in the contact areas. With further compression one or more distinct cracks ran through the specimen. Clearly, the structured mesh prescribes the fracture path. Nonetheless, for reasons stated above, see Section 2.2.3, no tetrahedron meshes can currently be used.

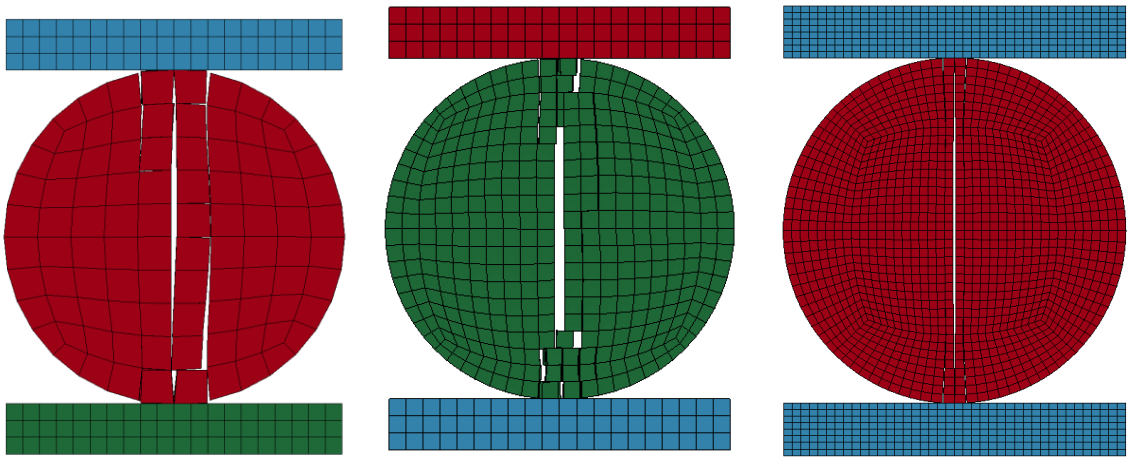

hex 0.01 hex 0.005 hex 0.0025

Figure 5 – Fracture paths for models with different meshes

Regarding peak forces levels, a strong dependency on the peak traction is observed (as expected). According to this result, the peak traction was adjusted for each mesh to achieve the measured forces. The resulting forces and used peak tractions for the **MAT_COHESIVE_ELASTIC** are shown in Figure 6. In addition, the forces were strongly dependent on the contact algorithm used. The **ERODING_SINGLE_SURFACE SOFT=2** formulation with **SBOPT=5 DEPTH=35** showed the best behavior. A coefficient of friction between ice and ice of 0.1 and between steel and ice of 0.03 is assumed. As the element size increases, the required peak traction of the CZM element decreases significantly.

The force curves of all simulations are shown in Figure 6. All simulations showed a brittle failure behavior. The overall stiffness of the finer meshes was less compared to the mesh with an element length of 0.01 m. During loading, the test specimen oscillates between the two load plates in the simulation. The load curve of the mesh with an element edge length of 0.0025 m changed from a force of approximately 1 kN because horizontal elements eroded in the contact area, which in turn lead to oscillations due to the contact algorithm.

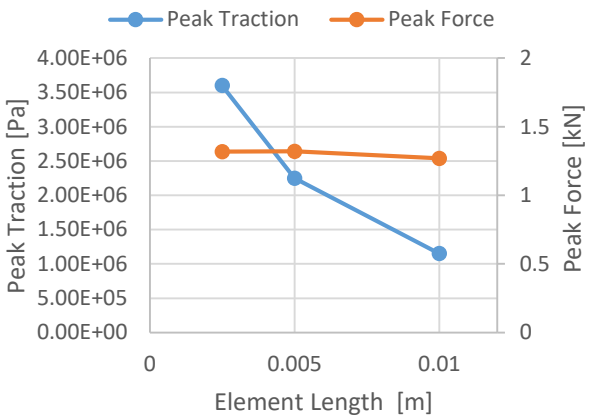

Figure 6 – Peak traction of cohesive elements (left y-axis) and peak force (right y-axis) in the simulations

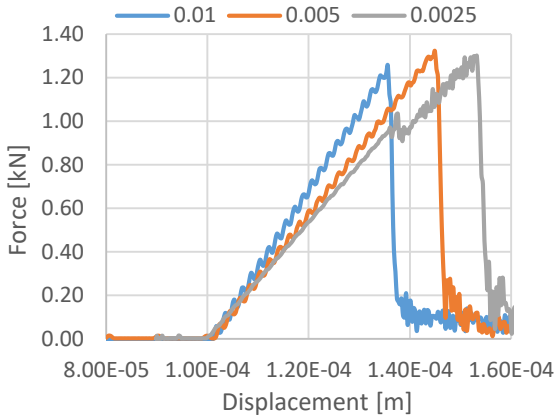

Figure 7 – Force between steel plates and specimen over time for different discretizations

4 Discussion and conclusion

The CZM in combination with an elastic bulk material is suitable for modeling of brittle behavior of ice. The validation and verification of the tensile splitting test simulations was mostly sucessful. A specific parameter set has to be identified for every model in dependence of the mesh. Regarding elastic parameters, this can be achieved with the approach given in Section 2.2. However, the calibration of other parameters such as the traction requires several simulation runs and remains to be time consuming.

Numerical stability is an issue. With the current approach, only using **`*MAT_COHESIVE_ELASTIC`** instead of **`*MAT_COHESIVE_MIXED_MODE`** yielded consistent results. The contact algorithm also proved to significantly influence the results. Such numerical issues also render automated calibration difficult.

Next, it is currently not possible to meet all model and parameter requirements indicated in Figure 2. Particularly the requirement for 2-3 elements in the process zone cannot be met with the current approach due to numerical instabilities for a fine mesh. On the other hand, coarse meshes appear to ‘swallow’ peak stresses which could be one reason for the requirement of higher tractions for coarser meshes.

Besides the numerical aspects it is concluded that tensile splitting tests are generally suited for the verification of fracture models for ice. This is true both from the numerical as well as the experimental perspective.

5 Acknowledgements

This work was supported by the US Office of Naval Research Global (ONRG) under NICOP Grant N62909-18-1-2127. We would also like to thank the German Federal Ministry for Economic Affairs and Energy (BMWi) for funding this research under the project reference number 0324022B and acknowledge the financial support of the Lloyd’s Register Foundation within the “Recommended practice of scenario based risk management for polar waters”. Lloyd’s Register Foundation helps to protect life and property by supporting engineering-related education, public engagement and the application of research. It is stated that all funders are not responsible for any of the content of this publication.

6 References

[1] R. Gagnon, “A numerical model of ice crushing using a foam analogue,” *Cold Regions Science and Technology*, vol. 65, no. 3, pp. 335–350, 2011.

[2] P. Moore, I. Jordaan, and R. Taylor, “Explicit Finite Element Analysis of Compressive Ice Failure Using Damage Mechanics,” in *Proceedings of the 22th International Conference on Port and Ocean Engineering under Arctic Conditions*, Espoo, 2013.

[3] A. Derradji-Aouat and Wang J., “Implementation, Verification and Validation of the Multi-Surface Failure Envelope for Ice in Explicit FEA (LS-DYNA) with Full Derivation of it’s

Invariant Form: Technical Report," NRC Institute for Ocean Technology, St. John's, 2009.
[4] Z. Liu, J. Amdahl, and S. Løset, "Plasticity based material modelling of ice and its application to ship–iceberg impacts," *Cold Regions Science and Technology*, vol. 65, no. 3, pp. 326–334, 2011.
[5] I. Gribanov, R. Taylor, and R. Sarracino, "Cohesive zone micromechanical model for compressive and tensile failure of polycrystalline ice," *Engineering Fracture Mechanics*, 2018.
[6] K. Kolari, "A complete three-dimensional continuum model of wing-crack growth in granular brittle solids," *International Journal of Solids and Structures*, vol. 115-116, pp. 27–42, 2017.
[7] L. Kellner *et al.,* "Establishing a common database of ice experiments and using machine learning to understand and predict ice behavior," *Cold Regions Science and Technology*, 2019.
[8] D. Iliescu and E. Schulson, "The brittle compressive failure of fresh-water columnar ice loaded biaxially," *Acta Materialia*, vol. 52, no. 20, pp. 5723–5735, 2004.
[9] H. Herrnring, L. Kellner, J. Kubiczek, and S. Ehlers, "Simulation of Ice-Structure Interaction with CZM-Elements," in *Proceedings of the 18th German LS-Dyna Forum*, Bamberg, Germany, 2018.
[10] J. Currier and E. Schulson, "The tensile strength of ice as a function of grain size," *Acta Metallurgica*, vol. 30, no. 8, pp. 1511–1514, 1982.
[11] R. Frederking, O. Svec, and G. Timco, "On measuring the shear strength of ice," in *Proceedings of the International Symposium on Ice*, Sapporo, Japan, 1988.
[12] Z. Kamio, H. Matsushita, and B. Strnadel, "Statistical analysis of ice fracture characteristics," *Engineering Fracture Mechanics*, vol. 70, no. 15, pp. 2075–2088, 2003.
[13] A. Tabiei and W. Zhang, "Cohesive element approach for dynamic crack propagation: Artificial compliance and mesh dependency," *Engineering Fracture Mechanics*, vol. 180, pp. 23–42, 2017.
[14] M. Mellor and I. Hawkes, "Measurement of Tensile Strength by diametral Compression of Discs and Annuli," *Engineering Geology*, 1971.
[15] *StandardTest Method for Splitting Tensile Strength of Intact Rock Core Specimens*, D3967 − 08, 2008.
[16] *Testing hardened concrete – Part 6: Tensile splitting strength of test German version EN 12390-6:2009*, 12390-6:2009, 2010.
[17] C. Dávila and P. Camanho, "Decohesion Elements using Two and Three-Parameter Mixed Mode Criteria," in *American Helicopter Society Conference*, Williamsburg, VA, 2001.
[18] A. Elvin, "Number of grains required to homogenize elastic properties of polycrystalline ice," *Mechanics of Materials*, vol. 22, no. 1, pp. 51–64, 1996.
[19] J. Dempsey, S. DeFranco, R. Adamson, and S. Mulmule, "Scale effects on the in-situ tensile strength and fracture of ice.: Part I: Large grained freshwater ice at Spray Lakes Reservoir, Alberta," in *Fracture Scaling*, Z. Bažant and Y. Rajapakse, Eds., Dordrecht: Springer Netherlands, 1999, pp. 325–345.
[20] S. Mulmule and J. Dempsey, "A Viscoelastic Fictitious Crack Model for the Fracture of Sea Ice," *Mechanics of Time-Dependent Materials*, vol. 1, no. 4, pp. 331–356, 1997.
[21] S. Mulmule and J. Dempsey, "Scale effects on sea ice fracture," *Mech. Cohes.-Frict. Mater.*, vol. 4, no. 6, pp. 505–524, 1999.
[22] J. Dempsey, D. Cole, and S. Wang, "Tensile fracture of a single crack in first-year sea ice," (eng), *Philosophical transactions. Series A, Mathematical, physical, and engineering sciences*, vol. 376, no. 2129, 2018.
[23] A. Fantilli, B. Chiaia, and B. Frigo, "Analogies in Fracture Mechanics of Concrete, Rock and Ice," *Procedia Materials Science*, vol. 3, pp. 397–407, 2014.
[24] J. Dempsey, "Scale Effects on the Fracture of Ice," in *The Johannes Weertman Symposium*, 1996.

[25] G. Timco and W. Weeks, “A review of the engineering properties of sea ice,” *Cold Regions Science and Technology*, vol. 60, no. 2, pp. 107–129, 2010.
[26] A. Turon, C. Dávila, P. Camanho, and J. Costa, “An engineering solution for mesh size effects in the simulation of delamination using cohesive zone models,” *Engineering Fracture Mechanics*, vol. 74, no. 10, pp. 1665–1682, 2007.
[27] J. Rice, “The Mechanics of Earthquake Rupture,” in *Proceedings of the International School of Physics "Enrico Fermi"*, vol. 78, *Physics of the earth's interior*, A. Dziewonski and E. Boschi, Eds., Amsterdam: North-Holland Publ. Co, 1980.
[28] M. Falk, A. Needleman, and J. Rice, “A critical evaluation of cohesive zone models of dynamic fracture,” *J. Phys. IV France*, vol. 11, no. PR5, Pr5-43-Pr5-50, 2001.
[29] N. Blal, L. Daridon, Y. Monerie, and S. Pagano, “Micromechanical-based criteria for the calibration of cohesive zone parameters,” *Journal of Computational and Applied Mathematics*, vol. 246, pp. 206–214, 2013.